

## Scaling structures of fluctuation spectra near chaotic transition points

H. Fujisaka, R. Hagihara, and M. Inoue

*Department of Physics, Kagoshima University, Kagoshima 890, Japan*

(Received 29 February 1988)

The symmetry dynamics and the fluctuation dynamics for local expansion rates are investigated in the vicinity of two kinds of intermittency transition points. This is done with the aid of the characteristic function  $\lambda_q$  and the fluctuation spectrum  $\sigma(\alpha)$  describing the global characteristics of time series. In both cases they obey the scaling laws  $\lambda_q = \epsilon^\mu L(q/\epsilon^\nu)$  and  $\sigma(\alpha) = \epsilon^{\mu+\nu} S(\alpha/\epsilon^\mu)$ , where  $\epsilon$  is the deviation from the transition point, and  $L$  and  $S$  are the scaling functions,  $\mu$  and  $\nu$  being constants.

### I. INTRODUCTION

The multifractal theory of strange attractors<sup>1</sup> is one of the main topics of recent studies on chaotic dynamics. This is essentially based on the Renyi exponent (dimension)  $D_q$  (Ref. 2) which was first applied to chaotic dynamics by Hentschel and Procaccia<sup>3(a)</sup> and Grassberger.<sup>3(b)</sup> The multifractal theory aims at global characterization for the cell to cell fluctuations of the probability exponents on the strange attractor. A similar global characterization of fluctuations has already been proposed a few years ago in the context of the velocity structure functions in the fully developed turbulence.<sup>4</sup> On the other hand, an approach to the global characterization of chaotic time series was developed by the present authors with the aid of the characteristic function  $\lambda_q$ .<sup>5,6</sup>

Recently, it became clear that  $D_q$  has close connection<sup>7</sup> in some cases with the characteristic exponent describing the fluctuations of local expansion rates (LER's).<sup>8-10</sup> This interrelation between  $D_q$  and LER's suggests the possibility of the unified treatment of the global characterization of fluctuations. One attempt has already been carried out by the present authors from the viewpoint of the self-similarity of relevant fluctuations.<sup>6</sup> We have shown that this straightforwardly leads to the fluctuation spectrum concept and the statistical-thermodynamics formalism.<sup>6</sup> Very recently Paladin and Vulpiani<sup>11</sup> have also proposed a similar unified treatment of multifractal phenomena in various systems.

Imagine a steady time series

$$\{u_n\} \equiv u_1, u_2, u_3, \dots \quad (1.1)$$

Our fluctuation spectrum theory<sup>6</sup> concerns how the local time average

$$\alpha_n = \frac{1}{n} \sum_{j=1}^n u_j \quad (1.2)$$

approaches the long-time average  $\alpha_\infty = \lim_{n \rightarrow \infty} n^{-1} \sum_{j=1}^n u_j$ , which is no longer a fluctuating variable, being assumed to be identical to the ensemble average of  $u_j$ . Even if  $n$  is sufficiently large, however,  $\alpha_n$  is still a fluctuating quantity. The fluctuation spectrum gives information about (i) the possible fluctuation range

of  $\alpha_n$  for a large  $n$  and (ii) the realization probability of the fluctuation.

The purpose of the present paper is to discuss the critical behavior of characteristic functions [Eq. (2.1)] and fluctuation spectra for the dynamics near two kinds of intermittency transition points, i.e., (a) the symmetry dynamics near the breakdown of chaos symmetry,<sup>12</sup> and (b) the fluctuation dynamics of local expansion rates near the type-I intermittency transition point.<sup>13</sup> The present paper is constructed as follows. In Sec. II we briefly describe the fluctuation spectrum theory of a time series. We shall study the critical behaviors for case (a) in Sec. III and case (b) in Sec. IV from the scaling structure standpoint. In Sec. V, we give a summary and remarks.

### II. FLUCTUATION SPECTRUM THEORY OF TIME SERIES

For a steady time series (1.1), the reduction of the fluctuations of the local time average (1.2) is evaluated by observing how the probability density  $\rho_n(\alpha')$  that  $\alpha_n$  takes values between  $\alpha'$  and  $\alpha' + d\alpha'$  approaches  $\delta(\alpha' - \alpha_\infty)$  as  $n \rightarrow \infty$ . Let us define the characteristic function  $\lambda_q$  by<sup>5</sup>

$$\lambda_q = \frac{1}{q} \lim_{n \rightarrow \infty} \frac{1}{n} \ln \langle \exp(qn\alpha_n) \rangle, \quad (2.1)$$

( $d\lambda_q/dq \geq 0$ ),  $\langle \rangle$  being the ensemble average. Then the fluctuation spectrum  $\sigma(\alpha')$ , defined through the assumption<sup>6</sup>

$$\rho_n(\alpha') \sim e^{-\sigma(\alpha')n}, \quad (2.2)$$

is shown to be related to  $\lambda_q$  as<sup>6</sup>

$$\lambda_q = -\frac{1}{q} \min_{\alpha'} [\sigma(\alpha') - q\alpha'] \quad (2.3)$$

by employing the saddle-point technique. This is equivalent to the Legendre transform

$$\alpha = \frac{d(q\lambda_q)}{dq}, \quad \sigma(\alpha) = q^2 \frac{d\lambda_q}{dq}. \quad (2.4)$$

We have noticed that<sup>6</sup>

$$\frac{d\alpha}{dq} \geq 0, \quad \frac{d^2\sigma(\alpha)}{d\alpha^2} > 0. \quad (2.5)$$

The fluctuation spectrum  $\sigma(\alpha)$  has a single minimal value  $\sigma=0$  at  $\alpha=\alpha_\infty(=\lambda_0=\langle u_n \rangle)$ .

If we expand (2.1) in the series of cumulants, the expansion converges for  $|q| < \kappa$ ,  $\kappa$  being the convergence radius. The  $\kappa$  separates three typical regions of  $q$ , ( $q \ll -\kappa$ ,  $|q| \ll \kappa$ ,  $q \gg \kappa$ ) as follows.<sup>5</sup> For  $|q| \ll \kappa$ ,  $\lambda_q$  can be approximately written as

$$\lambda_q = \lambda_0 + Dq, \quad (2.6)$$

where  $D = C_0/2 + \sum_{n=1}^{\infty} C_n$ ,  $C_n \equiv \langle u_n u_0 \rangle - \lambda_0^2$  being the double-time correlation function. The quantity  $D$  is related to the variance of  $\alpha_n$  as

$$\langle (\alpha_n - \alpha_\infty)^2 \rangle \simeq \frac{2D}{n} \quad (2.7)$$

for a large  $n$ , and has the meaning of the diffusion coefficient.<sup>5</sup> The asymptotic law (2.6) leads to

$$\alpha = \lambda_0 + 2Dq, \quad (2.8)$$

$$\sigma(\alpha) = \frac{(\alpha - \lambda_0)^2}{4D}. \quad (2.9)$$

The parabola (2.9) agrees with the central limit theorem result and is valid for  $|\alpha - \lambda_0| \ll |\alpha(q=\kappa) - \lambda_0|$ . On the other hand, for  $\theta q \gg \kappa$ , ( $\theta = \pm$ ), we generally get

$$\lambda_q \simeq \lambda_{\theta\infty} - \frac{1}{q} \left[ \frac{1}{\tau_\theta} - c_\theta \exp(-\eta_\theta |q|) \right], \quad (2.10)$$

where  $\tau_\theta$ ,  $c_\theta$ , and  $\eta_\theta$  are positive constants. Its Legendre transformation gives

$$\alpha \simeq \lambda_{\theta\infty} - \theta c_\theta \eta_\theta \exp(-\eta_\theta |q|), \quad (2.11)$$

$$\sigma(\alpha) \simeq \frac{1}{\tau_\theta} - \frac{1}{\eta_\theta} |\alpha - \lambda_{\theta\infty}| \ln \left[ \frac{a_\theta}{|\alpha - \lambda_{\theta\infty}|} \right], \quad (2.12)$$

where  $\eta_\theta \sim O(1/\kappa)$  and  $a_\theta \equiv e c_\theta \eta_\theta$ . The derivative  $d\sigma(\alpha)/d\alpha$  logarithmically diverges as  $\alpha \rightarrow \lambda_{\theta\infty}$ .

The existence of three characteristic regions of  $q$  is mathematically due to the finiteness of the convergence radius  $\kappa$ . As was shown in Ref. 5, on the other hand, its physical reason is the nonperturbative disconnectivity among the diffusion characteristic for  $|q| \ll \kappa$  and the two intermittency characteristics for  $|q| \gg \kappa$ .

Near chaotic transition points,  $\lambda_q$  often obeys the scaling laws of the form  $\lambda_q = \kappa^\mu F(q/\kappa)$ ,<sup>14-17</sup> where  $\mu$  is a constant and  $F(x)$  is a scaling function. Combining this with (2.4) leads to  $\sigma(\alpha) = \kappa^{\mu+1} G(\alpha/\kappa^\mu)$  with  $G(y) = \xi^2 dF(\xi)/d\xi$ , where  $\xi(y)$  is the inverse function of  $y = d[\xi F(\xi)]/d\xi$ . In the following sections, utilizing concrete models of two types of intermittency transitions, we shall determine explicit forms of  $F$  and  $G$ .

### III. DYNAMICS ASSOCIATED WITH BREAKDOWN OF CHAOS SYMMETRY

A typical example of the dynamics associated with the breakdown of the chaos symmetry is the band-splitting phenomenon observed in a wide range of chaotic phenomena.<sup>12,15,16,18</sup> The model we employ here is the one-dimensional mapping system  $x_{n+1} = f(x_n)$  with<sup>12</sup>

$$f(x) = \frac{1}{2} \sin \{ [2\pi + 2 \sin^{-1}(2\epsilon)] x \} \quad (|x| < \frac{1}{2}). \quad (3.1)$$

This has the inversion symmetry,  $f(-x) = -f(x)$ . When the control parameter  $\epsilon$  is positive, there exist migration channels connecting two regions  $x < 0$  and  $x > 0$ . For  $\epsilon < 0$ , migration channels disappear and the phase point is located in one of regions  $x < 0$  and  $x > 0$ . The location of the phase point is uniquely determined by the initial condition. Since the migration channels are narrow slightly above the threshold  $\epsilon=0$ , the average duration in each region is long for  $\epsilon \gtrsim 0$ . The long duration causes the intermittency concept.<sup>12</sup> Of course the present intermittency is different from those by Manneville and Pomeau.<sup>13</sup> Such symmetry dynamics is studied by observing the temporal evolution of the coarse-grained variable<sup>15,16</sup>

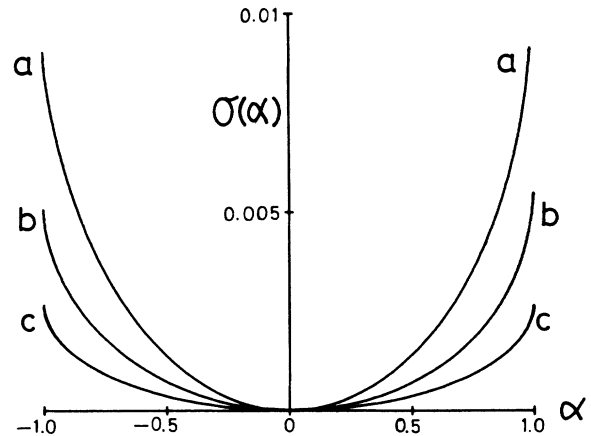
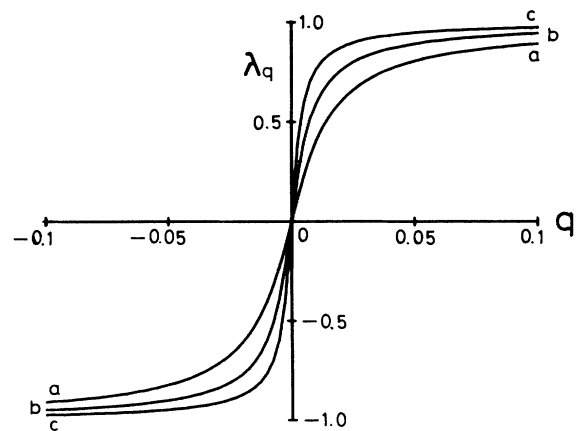


FIG. 1. Numerical results of the characteristic functions and the fluctuation spectra for the symmetry dynamics near the band-splitting point of the model (3.1). The  $\sigma(\alpha)$ 's were obtained by the numerical derivative of  $\lambda_q$ . Parameter values are  $\epsilon = 4 \times 10^{-4}$  (a),  $10^{-4}$  (b), and  $2 \times 10^{-5}$  (c). As  $\epsilon \rightarrow 0$ , the staircase structure of  $\lambda_q$  develops. Consequently, the parabolic structure of  $\sigma(\alpha)$  diminishes.

$$u_n = \begin{cases} 1 & (x_n > 0) \\ -1 & (x_n < 0) \end{cases} \quad (3.2)$$

The numerical results for the characteristic functions and the fluctuation spectra are shown in Fig. 1. As  $\epsilon \rightarrow 0$ , the slope  $D = d\lambda_q/dq|_{q=0}$  becomes steep as<sup>16</sup>

$$D \propto 1/\sqrt{\epsilon} \quad (3.3)$$

This is due to the elongation of the characteristic time near  $\epsilon=0$ . Namely, since  $D \sim \tau$ , the correlation time  $\tau$  being inversely proportional to the migration probability per unit step, we have  $D \sim \tau \sim 1/l\rho$ , where  $l$  is the width of the migration channel ( $l \sim \sqrt{\epsilon}$ ) and  $\rho [\sim O(\epsilon^0)]$  is the probability density at extrema of the map.<sup>16</sup> This gives (3.3). Simultaneously the staircase structure develops as  $\epsilon \rightarrow 0$ ,  $\lambda_{\pm\infty} (\simeq \pm 1)$  being insensitive to  $\epsilon$ , and the concave structure of  $\sigma(\alpha)$  tends to diminish. For  $\epsilon=0+$ ,  $\sigma(\alpha)$  lies on the  $\alpha$  axis, i.e.,  $\sigma(\alpha)=0$  for  $|\alpha| \leq 1$ , which is the alternative representation of the fully developed staircase structure of  $\lambda_q$ . For  $\epsilon < 0$ , the phase point is trapped in one of regions  $x < 0$  and  $x > 0$ , and  $\sigma(\alpha)=0$  at either  $\alpha=+1$  or  $-1$  according to the position of the phase point. Except for that point with  $\sigma=0$ , we obtain  $\sigma = \infty$ . This successive change of the fluctuation spectrum is characteristic of a symmetry-breaking transition.

Let us turn to the determination of the approximate forms of  $\lambda_q$  and  $\sigma(\alpha)$ . The dynamics for  $\epsilon \gtrsim 0$  yields  $\lambda_{-q} = -\lambda_q$ . So  $d\lambda_q/dq$  is an even function of  $q$ , being expanded as

$$\frac{d\lambda_q}{dq} = D \left[ 1 - \left( \frac{q}{q_*} \right)^2 + \dots \right], \quad (3.4)$$

if  $|q|$  is appropriately small, where we have noticed that the  $q^2$  term in  $d\lambda_q/dq$  acts so as to suppress the relation  $d\lambda_q/dq = D$  near  $q=0$  as  $q$  is increased. On the other hand,  $d\lambda_q/dq$  should be proportional to  $q^{-2}$  for a large  $q$  [Eq. (2.10)]. One simple interpolation approximation satisfying these requirements is to put

$$\frac{d\lambda_q}{dq} \simeq \frac{D}{1 + (q/q_*)^2} \quad (3.5)$$

The integration of (3.5) with the boundary condition  $\lambda_\infty \simeq 1$  leads to<sup>14-16</sup>

$$q_* = \frac{2}{\pi D}, \quad (3.6)$$

$$\lambda_q = \frac{2}{\pi} \tan^{-1} \left[ \frac{q}{q_*} \right] \quad (3.7)$$

The parameter  $q_*$  estimates the width of the  $q$  region satisfying  $\lambda_q \simeq \lambda_0 + Dq$ . Namely,  $q_*$  is roughly equal to the convergence radius of the expansion (3.4). The fluctuation spectrum  $\sigma(\alpha)$  is obtained by the Legendre transform as

$$\alpha = \frac{2}{\pi} \left[ \tan^{-1} \left[ \frac{q}{q_*} \right] + \frac{q/q_*}{1 + (q/q_*)^2} \right], \quad (3.8)$$

$$\frac{\sigma(\alpha)}{q_*} = \frac{2}{\pi} \frac{1}{1 + [I(\alpha)]^{-2}}, \quad (3.9)$$

where  $I(\alpha)$  is the solution of (3.8),  $[q/q_* = I(\alpha)]$ . The characteristic times  $\tau_{\pm}$  [Eqs. (2.10) and (2.12)] are thus evaluated as  $\tau_{\pm} = \pi^2 D / 4 \simeq 2.47D$ .

In a previous paper,<sup>16</sup> on the other hand, we have derived another scaling form of  $\lambda_q$ , which is regarded as the mean-field treatment result in the equilibrium critical phenomena. The result is

$$\lambda_q = \frac{\pi q_*}{4q} \ln \cosh \left[ \frac{4q}{\pi q_*} \right] \quad (3.10)$$

Its Legendre transform yields

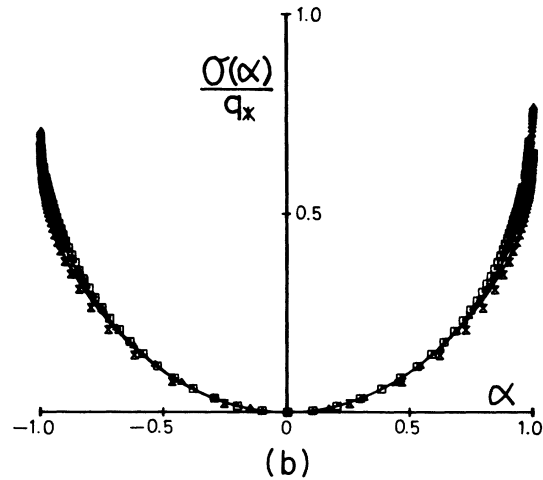
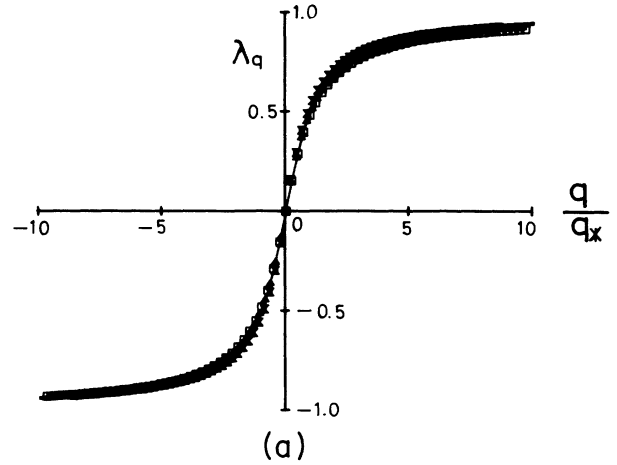


FIG. 2. Scaling relations of characteristic functions and fluctuation spectra shown in Fig. 1. Symbols  $\square$ ,  $\triangle$ , and  $\times$  are the results of a, b, and c in Fig. 1, respectively. The quantities  $q_*$  have been calculated by (3.6). Phenomenological scaling functions (3.7), (3.9), (3.10), and (3.12) are denoted by solid lines. The two approximations give quite similar results. We obtain excellent agreement between theoretical results and numerical ones over all regions of  $q$  and  $\alpha$ .

$$\alpha = \tanh \left( \frac{4q}{\pi q_*} \right), \quad (3.11)$$

$$\frac{\sigma(\alpha)}{q_*} = \frac{\pi}{8} [(1+\alpha) \ln(1+\alpha) + (1-\alpha) \ln(1-\alpha)]. \quad (3.12)$$

These scaling functions are characteristic of the coin tossing. The  $\tau_{\pm}$  are evaluated as  $\tau_{\pm} = 2D / \ln 2 \simeq 2.89D$ .

Thus we have two types of approximate analytic scaling expressions as  $\lambda_q = F_1(q/q_*)$  and  $\sigma(\alpha)/q_* = G_1(\alpha)$ . Numerical results given in Fig. 1 are plotted in the scaling forms in Fig. 2.  $\lambda_q$  and  $\sigma(\alpha)$  exhibit the scaling behaviors and both approximate scaling functions given above are in excellent agreement with numerical results.

#### IV. FLUCTUATION DYNAMICS OF LOCAL EXPANSION RATES

In this section we discuss the fluctuation dynamics of LER's near the type-I intermittency transition.<sup>13</sup> The fluctuations of LER's slightly above the type-I intermittency transition are due to both stochastic insertion of bursts among long ordered laminar regions and a trajectory instability in laminar regions. We use the one-dimensional intermittency model of So and Mori<sup>19</sup>  $x_{n+1} = f(x_n)$  with

$$f(x) = \begin{cases} f_l(x) \equiv x^2 + \frac{1}{4} + \epsilon & (0 \leq x \leq c) \\ f_b(x) \equiv (-x+1)(1-b)/(1-c) + b & (c < x \leq 1) \end{cases}, \quad (4.1)$$

where  $c = \sqrt{(3/4) - \epsilon}$ , and  $b$  is a positive constant, being chosen as  $b = 0.3$  in the present paper.  $\epsilon$  is the control parameter and  $\epsilon = 0$  is the transition point. By putting  $x_n = y_n + \frac{1}{2}$ , (4.1) can be rewritten in the conventional form

$$y_{n+1} = y_n + y_n^2 + \epsilon \quad (4.2)$$

near  $y_n = 0$ . The fluctuations of LER's are observed by studying the time series

$$u_n = \ln |f'(x_n)| \quad (n = 0, 1, 2, 3, \dots) \quad (4.3)$$

$[f'(x) \equiv df(x)/dx]$ .

Numerical results of  $\lambda_q$  and  $\sigma(\alpha)$  are shown in Fig. 3. As the system approaches the transition point, the dispersion range of the characteristic function  $\lambda_q$  diminishes. Especially, the conventional Lyapunov exponent  $\lambda_0$  decreases as<sup>20</sup>

$$\lambda_0 \propto \sqrt{\epsilon}. \quad (4.4)$$

Furthermore, as  $\epsilon \rightarrow 0$ , (i) the spectrum boundary  $\alpha = \lambda_{-\infty}$  approaches zero, (ii) the width of the  $\alpha$  region where  $\sigma(\alpha)$  has a parabolic structure becomes narrow, and (iii) the height of  $\sigma(\alpha)$  decreases. The decrease of the height of  $\sigma(\alpha)$  indicates the elongation of characteristic times  $\tau_{\pm}$  [Eq. (2.12)]. The numerical observation suggests that the slope  $D$  shrinks, obeying the power law  $D \propto \epsilon^{\phi}$ , where  $\phi = 0.25 - 0.35$ , and that  $\lambda_{-\infty} \propto \sqrt{\epsilon}$ .

In order to study the scaling structures of  $\lambda_q$  and  $\sigma(\alpha)$ , let us first postulate that the scaling behavior

$$\lambda_q = \lambda_0 F_2 \left( \frac{q}{\kappa} \right) \quad (4.5)$$

holds for  $q$  except for a large- $q$  region.  $F_2(y)$  is the scaling function [ $F_2(0) = 1$ ], and  $\kappa$  estimates the convergence radius of the cumulant expansion. The estimation  $\lambda_{-\infty} = \lambda_0 F_2(-\infty) \sim \lambda_0$  agrees with the observation  $\lambda_{-\infty} \propto \sqrt{\epsilon}$ . Equation (4.5) can be generally expanded as<sup>5,6</sup>

$$\lambda_q \simeq \lambda_{-\infty} - \frac{1}{q} \left[ \frac{1}{\tau_-} - c_- \exp(\eta_- q) \right] \quad (4.6)$$

for  $-q \gg \kappa$  [Eq. (2.10)]. We further postulate that this asymptotic form is valid not only for  $-q \gg \kappa$  but also for

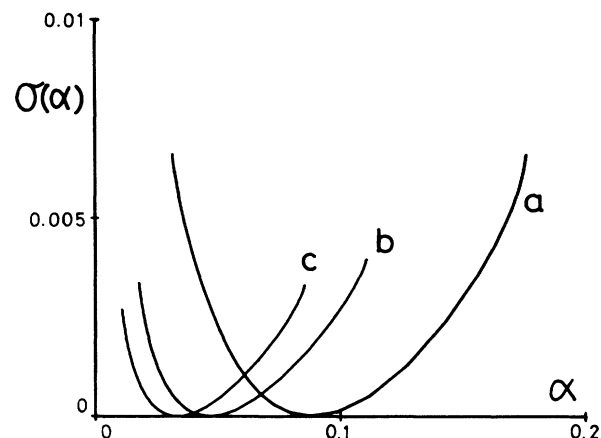
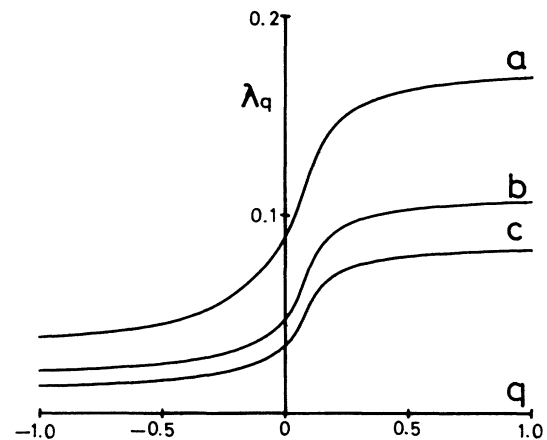


FIG. 3. Numerical results of  $\lambda_q$  and  $\sigma(\alpha)$  for the fluctuation dynamics of local expansion rates in the one-dimensional map (4.1) with  $b = 0.3$ . Parameter values are  $\epsilon = 5 \times 10^{-4}$  (a),  $1.25 \times 10^{-4}$  (b), and  $6.25 \times 10^{-5}$  (c). As  $\epsilon \rightarrow 0$ , the dispersion range of  $\lambda_q$  diminishes. Numerically we found  $\lambda_{-\infty} \simeq 0.35\lambda_0$ , ir- respectively for  $\epsilon$ .

$q < q_c$ ,  $q_c (> 0)$  being a certain characteristic value of  $q$ . Requiring that the above expansion gives (2.6) near  $q = 0$  determines the parameters as

$$\tau_1 = \frac{1}{c_-} = \frac{2D}{(\lambda_0 - \lambda_{-\infty})^2}, \tag{4.7a}$$

$$\eta_- = \frac{2D}{\lambda_0 - \lambda_{-\infty}} \equiv \frac{1}{\kappa}. \tag{4.7b}$$

Near  $\epsilon = 0$ , these are evaluated as  $\tau_- \propto \epsilon^{-0.7}$  and  $\kappa \propto \epsilon^{0.2}$ , provided that  $D \propto \epsilon^{0.3}$ , i.e.,  $\phi = 0.3$  is used. As is well known, the average duration  $n$  between successive bursts is estimated with (4.2), i.e.,  $y_n/n \sim y_n^2 \sim \epsilon$  as  $n \sim 1/\sqrt{\epsilon}$ .<sup>20</sup> However, the evaluation of the characteristic time  $\tau_-$  in  $\lambda_q$  for a large  $q$  gives  $\tau_- \propto \epsilon^{-0.7}$ . Since  $\lambda_{-\infty} \sim \sqrt{\epsilon}$ , we obtain

$$F_2(y) = r + (1-r)(e^y - 1)/y, \tag{4.8}$$

where  $r \equiv \lambda_{-\infty}/\lambda_0 [= F_2(-\infty)]$  is a numerical constant of order unity ( $0 < r < 1$ ). The scaling function  $(e^y - 1)/y$  is characteristic of the Poisson process. The Legendre transformation gives

$$\alpha = \lambda_0[r + (1-r)\exp(q/\kappa)]. \tag{4.9}$$

Accordingly the fluctuation spectrum obeys the scaling law

$$\frac{\sigma(\alpha)}{\lambda_0 \kappa} = G_2 \left( \frac{\alpha}{\lambda_0} \right), \tag{4.10}$$

where

$$G_2(y) = 1 - y + (y - r) \ln \left[ \frac{y - r}{1 - r} \right]. \tag{4.11}$$

The numerical observation suggests  $\lambda_q \sim \epsilon^\xi$  ( $\xi \simeq 0.3$ ) for a sufficiently large  $q$ . Evaluating  $q_c$ , the largest value of  $q$  where the asymptotic law (4.6) holds, through the matching condition  $\lambda_0 F_2(q_c/\kappa) \sim \lambda_{-\infty} \sim \epsilon^\xi$ , we find

$$q_c \simeq \kappa \ln \epsilon^{-1} \tag{4.12}$$

except for the numerical factor. Therefore we have two characteristic  $q$  regions. One is for  $q < q_c$ , where (4.5) and (4.6) hold. The magnitude of  $\lambda_q$  in this region is  $O(\sqrt{\epsilon})$ . The other is for  $q \gg q_c$ , where  $\lambda_q$  diminishes as  $\propto \epsilon^\xi$ . The ratio of  $\lambda_q$ 's in these regions is enhanced as  $\lambda_\infty/\lambda_{-\infty} \rightarrow \infty$ . We note that the region where (2.6) and (2.9) hold gradually shrinks as  $\epsilon \rightarrow 0$  because  $\kappa \sim \epsilon^{0.2}$ . Consequently, the boundary  $q_c$  approaches zero. However, since the ratio  $q_c/\kappa$  logarithmically diverges [Eq. (4.12)], the scaling relation  $\lambda_q/\lambda_0 = F_2(q/\kappa)$  tends to gradually cover the whole  $q/\kappa$  region as  $\epsilon \rightarrow 0$ .

In order to check the validity of (4.5) and (4.8), the numerical results in Fig. 3 are plotted in the scaling forms in Fig. 4, where we put  $r = 0.35$ . The theory explains numerical results fairly well for  $q/\kappa$  smaller than a crossover value. The crossover value gradually becomes large as  $\epsilon \rightarrow 0$ . This is compatible with the estimation  $q_c/\kappa \sim \ln \epsilon^{-1}$ . This agreement supports the validity of several postulations made above. Numerical results of  $\lambda_q$

in the large- $q$  region are extremely different from the theoretical result (4.5). Nevertheless, these differences do not appear in such a clear-cut way in the scaling form of  $\sigma(\alpha)$ . The fluctuation spectrum  $\sigma(\alpha)$  is in this way insensitive to observations or approximations in comparison with the characteristic function  $\lambda_q$ .

As is seen above, the approximation (4.6) is far from the numerical results for a large  $q$ . This suggests the existence of another scaling law valid for a large- $q$  region. Assume that there is no characteristic value of  $q$  except  $q_c$  which evaluates the region boundary between the Poissonian behavior and a large- $q$  behavior. So it is natural to scale  $q$  with  $q_c$ . Then the region boundary remains finite, independently of  $\epsilon$ , on the  $q/q_c$  line. If  $\lambda_q$  is scaled as  $\lambda_q/\lambda_\infty$ , then  $\lambda_q/\lambda_\infty$  for  $q/q_c > 1$  takes a finite value as  $\epsilon \rightarrow 0$ . On the other hand,  $\lambda_q/\lambda_\infty$  for  $q/q_c \ll 1$  approaches zero because  $\lambda_q \sim \epsilon^{0.5}$  for  $q < q_c$  and  $\lambda_\infty \sim \epsilon^{0.3}$ . Figure 5 shows the  $q/q_c$  versus  $\lambda_q/\lambda_\infty$  plot. The numerical observation seems to imply the scaling relation

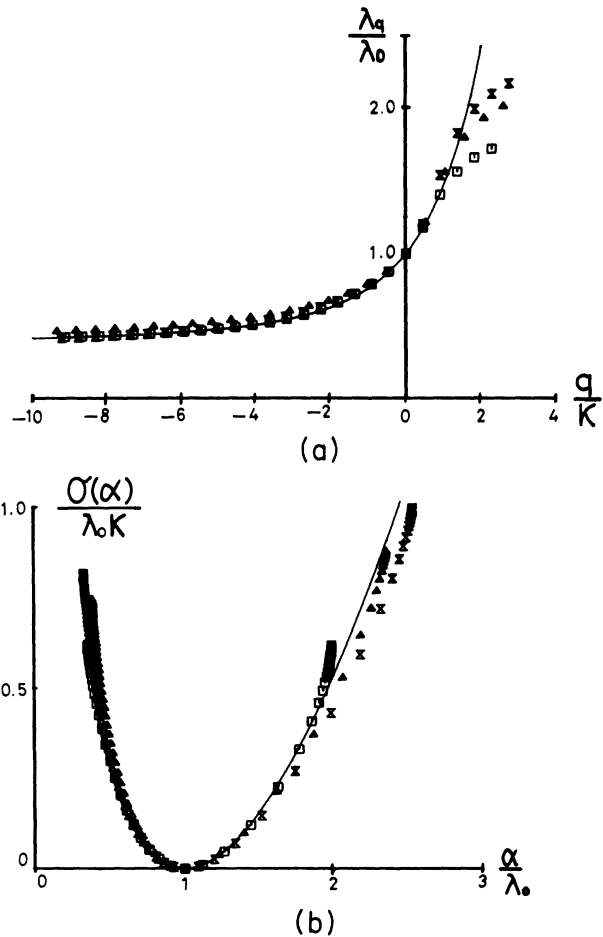


FIG. 4. Scaling behaviors of characteristic functions and fluctuation spectra given in Fig. 3. Symbols  $\square$ ,  $\triangle$ , and  $\times$  correspond to  $a$ ,  $b$ , and  $c$  in Fig. 3, respectively. Solid lines are theoretical results (4.5) and (4.8), where we have put  $r = 0.35$ . As  $\epsilon \rightarrow 0$ , the scaling region where (4.5) with (4.8) holds becomes wider on the  $q/\kappa$  axis.

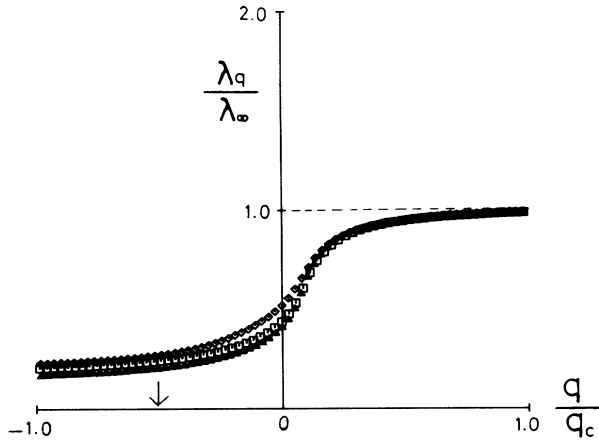


FIG. 5. Another scaling property observed for  $\lambda_q$  for the fluctuation dynamics of LER's. Parameter values are  $\epsilon=5 \times 10^{-4}$  ( $\diamond$ ),  $1.25 \times 10^{-4}$  ( $\square$ ), and  $6.25 \times 10^{-5}$  ( $\triangle$ ). As  $\epsilon \rightarrow 0$ ,  $\lambda_q/\lambda_\infty$  seems to approach zero for  $q/q_c \lesssim O(1)$  and a definite function of  $q/q_c$  for  $q/q_c \gtrsim O(1)$ . Such behavior is possible because the  $\lambda_q$ 's for  $q < q_c$  and  $q > q_c$  diminish in a different way, i.e.,  $\lambda_q \sim \epsilon^{0.5}$  for  $q < q_c$  and  $\sim \epsilon^{0.3}$  for  $q > q_c$ .

$$\frac{\lambda_q}{\lambda_\infty} = L_1 \left[ \frac{q}{q_c} \right] \quad [L_1(\infty) = 1] \quad (4.13)$$

holds, where  $L_1(y)$  is the scaling function. Since  $\lambda_0 \sim \epsilon^{0.5}$  and  $\lambda_\infty \sim \epsilon^{0.5}$ , one obtains  $L_1(y) \simeq 0$  for  $y \lesssim O(1)$ .<sup>21</sup> More generally speaking,  $\lambda_q/\lambda_\infty$  practically vanishes for  $q/q_c \lesssim O(1)$  ( $\simeq 0.1$ ), and it suddenly increases in a narrow region located at  $q/q_c \lesssim O(1)$  as  $q/q_c$  is changed from the left. Then it approaches unity for  $q/q_c \rightarrow \infty$ . Namely, the derivative  $d(\lambda_q/\lambda_\infty)/d(q/q_c)$  is expected to take a large value only in a narrow region of  $q/q_c$ . The Legendre transform of (4.3) leads to

$$\frac{\sigma(\alpha)}{\lambda_\infty q_c} = S_1 \left[ \frac{\alpha}{\lambda_\infty} \right], \quad (4.14)$$

with the scaling function  $S_1$ .

We therefore conclude that the present  $\lambda_q$  has two types of scaling structures. This originates from the fact that the characteristic function  $\lambda_q$  shrinks as  $\epsilon \rightarrow 0$  in a different way for  $q < q_c$  and  $q_c \ll q$ . Such a situation is different from the scaling structure observed in Sec. III in the symmetry dynamics associated with the breakdown of the chaos symmetry, where there is only one scaling relation governing the whole  $q$  region.

### V. SUMMARY AND REMARKS

In the present paper we studied the global statistical characteristics for (a) the dynamics associated with the breakdown of the chaos symmetry and (b) the fluctuation dynamics of local expansion rates, near their intermittency transitions. We have shown that in both cases the characteristic functions and the fluctuation spectra obey the scaling laws

$$\lambda_q = \Lambda_1(q/\epsilon^{1/2}), \quad \sigma(\alpha) = \epsilon^{1/2} \Sigma_1(\alpha), \quad (5.1)$$

for case (a), and

$$\lambda_q = \epsilon^{1/2} \Lambda_2(q/\epsilon^{(1/2)-\phi}), \quad \sigma(\alpha) = \epsilon^{1-\phi} \Sigma_2(\alpha/\epsilon^{1/2}), \quad (5.2)$$

( $\phi = 0.25 - 0.35$ ) for case (b). In contrast to that the scaling relation (5.1) holds over the whole  $q$  region, the relation (5.2) is valid for  $q/\epsilon^{(1/2)-\phi} \lesssim \ln \epsilon^{-1}$ . So in the limit  $\epsilon \rightarrow 0$ , the scaling law (5.2) tends to cover the whole  $q/\epsilon^{(1/2)-\phi}$  region. The  $\lambda_q$  for  $q/\epsilon^{(1/2)-\phi} \gtrsim \ln \epsilon^{-1}$ , on the other hand, exhibits another scaling structure. [See Eqs. (4.13) and (4.14).] Accordingly,  $\lambda_q/\lambda_\infty$  at  $\epsilon = 0+$  sharply changes from zero to unity in a narrow region  $q/q_c \simeq O(1)$  as  $q/q_c$  is increased from the negative- $q$  region. Namely, for  $q/q_c \lesssim O(1)$  there is no fluctuation globally detected through  $\lambda_q/\lambda_\infty$ . On the other hand, for  $q/q_c \gtrsim O(1)$ , it can be detected. Another simple example exhibiting such remarkable scaling behaviors is illustratively given in the Appendix.

As was shown in Ref. 22, in a one-dimensional map-

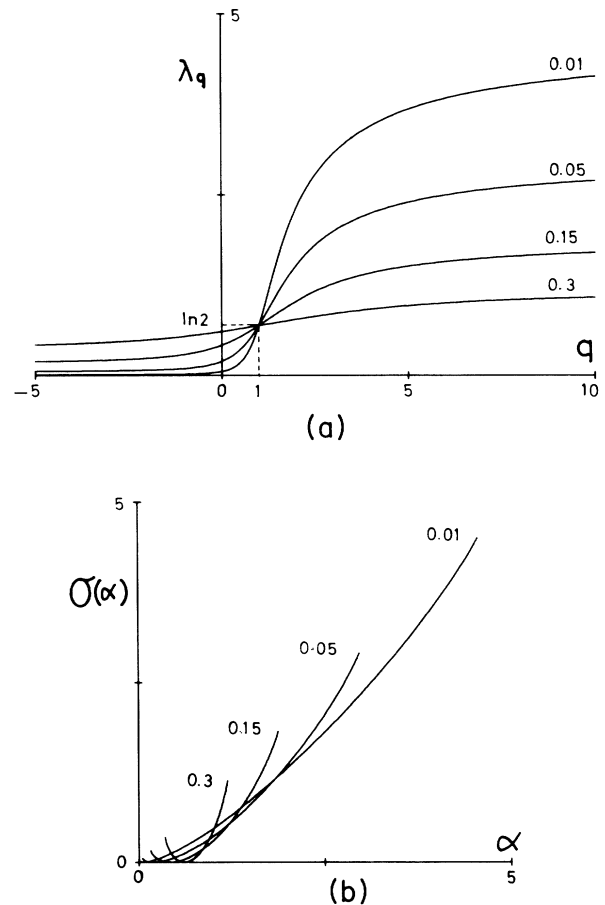


FIG. 6. Critical behaviors of  $\lambda_q$  and  $\sigma(\alpha)$  for the fluctuation dynamics of local expansion rates for the model (A2). The numerical values are those of  $p$ . As  $p \rightarrow 0$ ,  $\lambda_q$  strongly bends. Simultaneously the fluctuation range of  $\alpha$  becomes large.

ping system where  $u_n$  is a unique function of  $x_n$  as  $u_n = u(x_n)$  the characteristic function  $\lambda_q$  from the first principle is obtained by solving the eigenvalue equation<sup>22</sup>

$$H_q \psi_q^{(l)}(x) = \exp(-\zeta_q^{(l)}) \psi_q^{(l)}(x), \tag{5.3}$$

where  $H_q$  is defined by  $H_q F(x) = H[e^{qu(x)} F(x)]$  with the Frobenius-Perron operator  $H$ .<sup>23</sup> Namely,  $\lambda_q$  is determined by the largest eigenvalue of  $H_q$  as

$$\lambda_q = -\frac{1}{q} \min_l (\text{Re} \zeta_q^{(l)}). \tag{5.4}$$

The approximate expressions of scaling functions heuristically or phenomenologically obtained in the preceding sections are desirable to be justified by solving the eigenvalue equation (5.3).

In connection with the eigenvalue problem (5.3), let us make a comment on the temporal correlation in  $\{u_n\}$ . The characteristic function  $\lambda_q$  is alternatively defined by

$$\langle \exp(qn\alpha_n) \rangle = Q_n^{(q)} \exp(q\lambda_q n), \tag{5.5}$$

where  $Q_n^{(q)}$  satisfying

$$\lim_{n \rightarrow \infty} \frac{1}{n} \ln Q_n^{(q)} = 0 \tag{5.6}$$

is relevant to the temporal correlation embedded in  $\{u_n\}$ . By introducing the quantity

$$\Xi_q(\omega) = \sum_{n=0}^{\infty} Q_n^{(q)} \cos(\omega n), \tag{5.7}$$

its poles give the order- $q$  characteristic frequencies and damping rates.<sup>22,24</sup> All eigenvalues in (5.3) contribute to  $\Xi_q(\omega)$ , which contains information different from those in  $\lambda_q$ . In order to elucidate more precise statistical characteristics of  $\{u_n\}$ , we should go into the survey of  $\Xi_q(\omega)$ . Especially near the intermittency transitions, long-lived temporal correlations affect the shape of  $\Xi_q(\omega)$ . Further studies in this direction will be reported elsewhere.

ACKNOWLEDGMENTS

The authors thank Professor H. Mori, Dr. T. Yoshida, and Professor T. Yamada for continuous encouragement and helpful suggestions. This study was partially supported by a Grant-in-Aid for Scientific Research from the Ministry of Education, Science, and Culture, Japan.

APPENDIX

In this appendix we give another solvable, simple example exhibiting scaling behaviors similar to those observed in Sec. IV.

The time series under consideration is the fluctuation of LER's

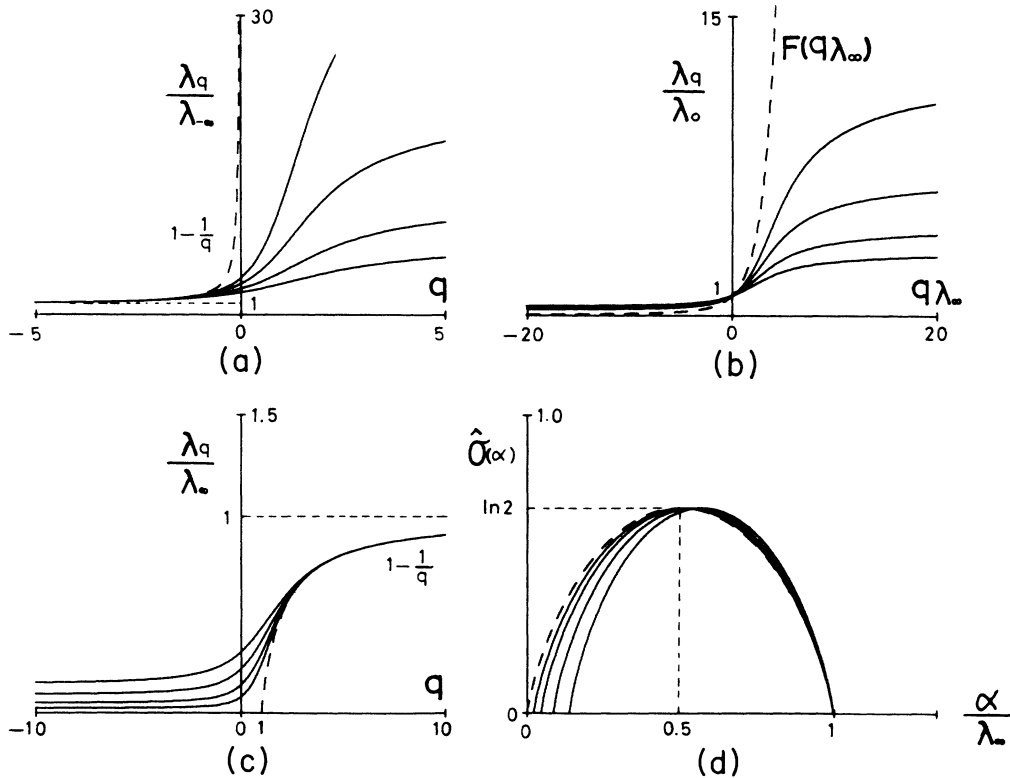


FIG. 7. Scaling plots of  $\lambda_q$  and  $\sigma(\alpha)$  for the fluctuation dynamics of local expansion of the model (A2) for  $p=0.2, 0.15, 0.1,$  and  $0.06$ . As  $p \rightarrow 0$ , the exact results monotonously approach the scaling functions (dashed lines) given in Eqs. (A9) and (A10). (c), especially, should be compared with the characteristics depicted in Fig. 5.

$$u_n = \ln |f'(x_n)| \quad (\text{A1})$$

for the one-dimensional map

$$x_{n+1} = f(x_n) = \begin{cases} x_n/p & (0 \leq x_n < p) \\ (x_n - p)/(1-p) & (p \leq x_n < 1) \end{cases} \quad (\text{A2})$$

( $0 < p < \frac{1}{2}$ ). The characteristic function  $\lambda_q$  is easily obtained as

$$\lambda_q = \frac{1}{q} \ln(e^{(q-1)\lambda_\infty} + e^{(q-1)\lambda_{-\infty}}), \quad (\text{A3})$$

where

$$\lambda_\infty = \ln p^{-1}, \quad \lambda_{-\infty} = \ln(1-p)^{-1}. \quad (\text{A4})$$

The Legendre transform of (A3) gives

$$\alpha = \frac{\lambda_\infty e^{(q-1)\lambda_\infty} + \lambda_{-\infty} e^{(q-1)\lambda_{-\infty}}}{e^{(q-1)\lambda_\infty} + e^{(q-1)\lambda_{-\infty}}}, \quad (\text{A5})$$

$$\sigma(\alpha) = \alpha - \hat{\sigma}(\alpha), \quad (\text{A6})$$

where

$$\hat{\sigma}(\alpha) = -(1-f_\alpha) \ln(1-f_\alpha) - f_\alpha \ln f_\alpha, \quad (\text{A7})$$

$$f_\alpha = \frac{\alpha - \lambda_{-\infty}}{\lambda_\infty - \lambda_{-\infty}}. \quad (\text{A8})$$

As  $p \rightarrow 0$ , the spectral structures of  $\lambda_q$  and  $\sigma(\alpha)$  are diminished for  $q < 1$  and are enhanced for  $q > 1$ ,  $\lambda_{q=1}$  taking the value  $\ln 2$  independently of  $p$  (Fig. 6). Such critical behaviors are studied by considering the asymptotic

forms of  $\lambda_q$  and  $\sigma(\alpha)$ . In the present model there exist three characteristic values of the fluctuation  $\alpha$  for  $p \rightarrow 0$ , i.e.,

$$\lambda_{-\infty}, \quad \lambda_0 [= p\lambda_\infty + (1-p)\lambda_{-\infty}], \quad \lambda_\infty.$$

The characteristic behaviors of fluctuations corresponding to them are described by the limiting laws

$$\lim_{p \rightarrow 0} \frac{\lambda_q}{\lambda_{-\infty}} = \begin{cases} 1 - q^{-1} & (q < 0) \\ +\infty & (q > 0), \end{cases} \quad (\text{A9a})$$

$$\lim_{p \rightarrow 0} \frac{\lambda_y/\lambda_\infty}{\lambda_0} = F(y) \quad (-\infty < q < \infty), \quad (\text{A9b})$$

$$\lim_{p \rightarrow 0} \frac{\lambda_q}{\lambda_\infty} = \begin{cases} 0 & (q \leq 1) \\ 1 - q^{-1} & (q > 1), \end{cases} \quad (\text{A9c})$$

where  $F(y) = (e^y - 1)/y$ . Such behaviors are drawn in Figs. 7(a)–7(c). Furthermore, Eq. (A7) is simply written as, for  $p \rightarrow 0$ ,

$$\hat{\sigma}(\alpha) = -(1-x) \ln(1-x) - x \ln x \equiv h(x), \quad (\text{A10})$$

where  $x = \alpha/\lambda_\infty$ . In Fig. 7(d),  $\hat{\sigma}(\alpha)$  [Eq. (A7)] is plotted as a function of  $\alpha/\lambda_\infty$  for several values of  $p$ . One observes that  $\hat{\sigma}(\alpha)$  approaches (A10) as  $p \rightarrow 0$ .

The present simple example exhibits several aspects similar to those found in Sec. IV. One of the important differences is that in comparison with the crossover value  $q_c$  in Sec. IV, which approaches zero as the system approaches the transition point, it takes unity ( $q_c = 1$ ) in the present model.

<sup>1</sup>See, e.g., T. C. Halsey, M. H. Jensen, L. P. Kadanoff, I. Procaccia, and B. I. Shraiman, *Phys. Rev. A* **33**, 1141 (1986).

<sup>2</sup>A. Renyi, *Probability Theory* (North-Holland, Amsterdam, 1970).

<sup>3</sup>(a) H. G. E. Hentschel and I. Procaccia, *Physica D* **8**, 435 (1983); (b) P. Grassberger, *Phys. Lett.* **97A**, 227 (1983).

<sup>4</sup>U. Frisch and G. Parisi, in *Turbulence and Predictability in Geophysical Fluid Dynamics and Climate Dynamics*, Proceedings of the International School of Physics "Enrico Fermi," Course LXXXVIII, Varenna, 1983, edited by M. Ghil, R. Benzi, and G. Parisi (North-Holland, New York, 1985), p. 84.

<sup>5</sup>H. Fujisaka, *Prog. Theor. Phys.* **71**, 513 (1984); H. Fujisaka and M. Inoue, *ibid.* **74**, 20 (1985); M. Inoue and H. Fujisaka, *ibid.* **77**, 1077 (1987).

<sup>6</sup>H. Fujisaka and H. Inoue, *Prog. Theor. Phys.* **77**, 1334 (1987).

<sup>7</sup>J.-P. Eckmann and I. Procaccia, *Phys. Rev. A* **34**, 659 (1986); M. Sano, S. Sato, and Y. Sawada, *Prog. Theor. Phys.* **76**, 945 (1986); R. Baddii and A. Politi, *Phys. Rev. A* **35**, 1288 (1987); *Phys. Scr.* **35**, 243 (1987); T. Yoshida and B. C. So, *Prog. Theor. Phys.* **79**, 1 (1988); T. Morita, H. Hata, H. Mori, T. Horita, and K. Tomita, *ibid.* **79**, 296 (1988).

<sup>8</sup>H. Fujisaka, *Prog. Theor. Phys.* **70**, 1264 (1983).

<sup>9</sup>R. Benzi, G. Paladin, G. Parisi, and A. Vulpiani, *J. Phys. A* **18**, 2157 (1984).

<sup>10</sup>T. Bohr and D. Rand, *Physica D* **25**, 387 (1987).

<sup>11</sup>G. Paladin and A. Vulpiani, *Phys. Rep.* **156**, 147 (1987).

<sup>12</sup>H. Fujisaka, H. Kamifukumoto, and M. Inoue, *Prog. Theor.*

*Phys.* **69**, 333 (1983), and references therein.

<sup>13</sup>P. Manneville and Y. Pomeau, *Physica D* **1**, 219 (1980).

<sup>14</sup>H. Fujisaka, M. Inoue, and H. Uchimura, *Prog. Theor. Phys.* **72**, 23 (1984); M. Inoue and H. Fujisaka, *Phys. Rev. B* **32**, 277 (1985); M. Inoue, T. Kawaguchi, and H. Fujisaka, *Phys. Lett. A* **115**, 139 (1986).

<sup>15</sup>H. Ishii, H. Fujisaka, and M. Inoue, *Phys. Lett. A* **116**, 257 (1986).

<sup>16</sup>H. Uchimura, H. Fujisaka, and M. Inoue, *Prog. Theor. Phys.* **77**, 1344 (1987).

<sup>17</sup>M. Inoue, H. Fujisaka, and O. Yamaki (unpublished).

<sup>18</sup>See also C. Grebogi, E. Ott, F. Romeiras, and J. A. Yorke, *Phys. Rev. A* **36**, 5365 (1987).

<sup>19</sup>B. C. So and H. Mori, *Prog. Theor. Phys.* **72**, 1258 (1984); *Physica D* **21**, 126 (1986).

<sup>20</sup>J. E. Hirsch, B. A. Huberman, and D. J. Scalapino, *Phys. Rev. A* **25**, 519 (1982).

<sup>21</sup>One clearly sees that numerical results of  $\lambda_q/\lambda_\infty$  for  $q \leq 0$  are still large. This comes because the rate  $\lambda_0/\lambda_\infty \sim \epsilon^{0.5}/\epsilon^{0.3} \sim \epsilon^{0.2}$  cannot be still negligible ( $\sim 10^{-1}$ ) even for  $\epsilon = 10^{-6}$ . However, we can expect that  $\lambda_q/\lambda_\infty$  approaches zero for  $q/q_c \lesssim O(1)$  as  $\epsilon \rightarrow 0$ .

<sup>22</sup>H. Fujisaka and M. Inoue, *Prog. Theor. Phys.* **78**, 268 (1987).

<sup>23</sup>Recently, a similar eigenvalue problem has been discussed by T. Tél, *Phys. Rev. A* **36**, 2507 (1987) on the basis of the work of P. Szépfalussy and T. Tél, *Phys. Rev. A* **34**, 2520 (1986).

<sup>24</sup>H. Fujisaka and M. Inoue, *Prog. Theor. Phys.* **78**, 1203 (1987).